Molecular Biology of the Cell
Vol. 12, 3759–3773, December 2001

Regulation of Yeast Actin Cytoskeleton-Regulatory Complex Pan1p/Sla1p/End3p by Serine/Threonine Kinase Prk1p

Guisheng Zeng, Xianwen Yu, and Mingjie Cai*

Institute of Molecular and Cell Biology, National University of Singapore, Singapore, 117609

Submitted April 5, 2001; Revised August 3, 2001; Accepted September 12, 2001
Monitoring Editor: Tim Stearns

The serine/threonine kinase Prk1p is known to be involved in the regulation of the actin cytoskeleton organization in budding yeast. One possible function of Prk1p is the negative regulation of Pan1p, an actin patch regulatory protein that forms a complex in vivo with at least two other proteins, Sla1p and End3p. In this report, we identified Sla1p as another substrate for Prk1p. The phosphorylation of Sla1p by Prk1p was established in vitro with the use of immunoprecipitated Prk1p and in vivo with the use of *PRK1* overexpression, and was further supported by the finding that immunoprecipitated Sla1p contained *PRK1*- and *ARK1*-dependent kinase activities. Stable complex formation between Prk1p and Sla1p/Pan1p in vivo could be observed once the phosphorylation reaction was blocked by mutation in the catalytic site of Prk1p. Elevation of Prk1p activities in wild-type cells resulted in a number of deficiencies, including those in colocalization of Pan1p and Sla1p, endocytosis, and cell wall morphogenesis, likely attributable to a disintegration of the Pan1p/Sla1p/End3p complex. These results lend a strong support to the model that the phosphorylation of the Pan1p/Sla1p/End3p complex by Prk1p is one of the important mechanisms by which the organization and functions of the actin cytoskeleton are regulated.

INTRODUCTION

The rapid assembly and disassembly of actin filaments at specific subcellular locations provide the mechanistic basis for various dynamic activities such as cell motility, change of cell shapes, and translocation of intracellular organelles (Carlier and Pantaloni, 1997; Mermall *et al.*, 1998; Cooper and Schafer, 2000). An important part of our current knowledge on the actin cytoskeleton dynamics comes from studies of the actin cytoskeleton organization in the yeast *Saccharomyces cerevisiae*. The major actin cytoskeletal structures in yeast are the cortical patches and the cytoplasmic cables, both of which display a conspicuous pattern of dynamics during the cell cycle. The pattern of cellular distribution of these actin structures has long been noticed to correlate with that of the localized surface growth (Adams and Pringle, 1984; Kilmartin and Adams, 1984; Novick and Botstein, 1985). The actin patches and cables are distributed evenly in unbudded cells undergoing isotropical surface expansion. At the time of bud emergence and during the entire period of bud formation, the yeast cell assumes an apical growth pattern, with most if not all of the actin patches mobilized first to the bud site and later in the bud. The mother cell exhibits essentially no enlargement during this time and contains only the actin cables, which are all aligned toward the bud (Adams and Pringle, 1984; Kilmartin and Adams, 1984; Lew and Reed, 1993). Despite the correlation in the patterns of actin distribution and bud formation, the exact roles of the actin cytoskeleton, especially the cortical patches, in promoting cell growth have remained largely unknown. Although cytoplasmic cables may serve as paths for myosin molecules to transport secretion vesicles to the cell surface (Novick and Botstein, 1985; Govindan *et al.*, 1995; Ayscough *et al.*, 1997; Pruyne *et al.*, 1998), a polarized distribution of the cortical patches does not appear to be a necessity for bud growth, because mutants that failed to maintain a polarized localization of the cortical actin patches could still form bud efficiently (Karpova *et al.*, 2000).

Among a large number of proteins that have been identified to play direct or indirect roles in the function of the actin cytoskeleton in yeast are a group of actin patch proteins (Pruyne and Bretscher, 2000). These proteins reside on the cell cortex as clusters and partially colocalize with the actin patches. Three of them, Pan1p, End3p, and Sla1p, have been known to form a complex in vivo (Tang *et al.*, 2000), and to be required for the actin patch morphology, membrane protein endocytosis, and cell wall synthesis (Holtzman *et al.*, 1993; Bénédetti *et al.*, 1994; Tang and Cai, 1996; Tang *et al.*, 1997, 2000; Ayscough *et al.*, 1999). Recently, the role of Pan1p

* Corresponding author. E-mail address: mcbcaimj@imcb.nus.edu.sg.

in the actin cytoskeleton organization and endocytosis has been suggested to be due to its ability to bind and activate the Arp2/3 complex (Duncan *et al.*, 2001). Two kinases, Prk1p and Ark1p, have been identified as regulatory factors in the actin cytoskeleton organization in yeast (Cope *et al.*, 1999; Zeng and Cai, 1999). Prk1p was discovered from a genetic screen as a possible negative regulator of Pan1p, because a loss-of-function mutation in *PRK1* suppressed the temperature sensitivity of the *pan1-4* mutant (Zeng and Cai, 1999). Combination of the *prk1* null mutation and *pan1-4* largely corrected the actin abnormalities in the *pan1-4* single mutant. At 37°C, the *prk1* null mutant was viable but was unable to maintain an asymmetric distribution of the actin patches (Zeng and Cai, 1999). On the other hand, overexpression of *PRK1* in wild-type cells led to lethality and gross actin cytoskeleton abnormalities (Zeng and Cai, 1999). In vitro kinase assays demonstrated that Prk1p was able to phosphorylate Pan1p specifically on the LxxQxTG motifs. Clearly, Prk1p is involved in a pathway of actin cytoskeleton regulation with Pan1p as a potential target. The function of Ark1p in the regulation of the actin cytoskeleton is less unveiled. Both Prk1p and Ark1p colocalize with the cortical patches (Cope *et al.*, 1999; Zeng and Cai, 1999).

In this study, we show that Sla1p is another regulatory target of Prk1p. Additional evidence is presented to support the proposal that Prk1p negatively regulates the Pan1p/Sla1p/End3p complex by affecting the complex formation between these proteins.

MATERIALS AND METHODS

Strains, Media, and General Methods

The yeast strains used in this study are listed in Table 1. Yeast cells were propagated in rich medium (YPD), synthetic complete medium (SC), or SC lacking the appropriate amino acids for plasmid maintenance (Rose *et al.*, 1990). In experiments requiring the expression of genes under the *GAL1* promoter, raffinose instead of dextrose was used as the carbon source and galactose was later added for *GAL1* induction. Genetic and recombinant DNA manipulations were performed according to standard methods (Sambrook *et al.*, 1989; Rose *et al.*, 1990).

Plasmid and Strain Constructions

The plasmid constructs used in this study are shown in Table 2. Disruption of the *PRK1* gene (*prk1*Δ*::URA3*) to generate YMC427 has been described previously (Zeng and Cai, 1999). To disrupt the *ARK1* gene, DNA fragment containing the opening reading frame of *ARK1* and the flanking sequences was cloned by polymerase chain reaction (PCR) into the vector pRS316. The *Hpa*I/*Bam*HI fragment of the resulting plasmid containing most of the *ARK1* coding sequence was then replaced with the *LEU2* gene. After digestion by *Sac*II-*Sal*I, the fragment containing *LEU2*-disrupted *ARK1* was transformed into W303-1B and YMC427 to generate YMC438 and YMC439, respectively. Deletion strains were confirmed by PCR analysis (Huxley *et al.*, 1990).

The strains YMC440 and YMC441 were generated by linearizing the plasmids pRS306-PAN1c-HA and pRS306-PAN1c-Myc within the *PAN1* gene by *Bam*HI and transforming the linearized plasmids into W303-1B and W303-1A, respectively. YMC442, YMC443, and YMC444 were generated by integrating the *Bam*HI-linearized pRS304-PAN1c-Myc into strains YMC427, YMC438, and YMC439, respectively. To obtain the strain YMC445, the *Sac*I-linearized pRS305-SLA1c-GFP and the *Bam*HI-linearized pRS304-PAN1c-RFP were integrated into W303-1A sequentially. All integration strains were confirmed by PCR analysis.

Table 1. Yeast strains used in this study

Strain	Genotype
W303-1A	*MAT***a** *ade2-1 trp1-1 can1-100 leu2-3,112 his3-11,15 ura3-1*
W303-1B	*MAT*α *ade2-1 trp1-1 can1-100 leu2-3,112 his3-11,15 ura3-1*
SFY526	*MAT***a** *ade2-101 trp1-901 can*^{r} *leu2-3,112 his3-200 ura3-52 lys2-801 gal4-542 gal80-538 URA3::GAL1-lacZ*
YMC427	*MAT***a** *ade2-1 trp1-1 can1-100 leu2-3,112 his3-11,15 ura3-1 prk1*Δ*::URA3*
YMC438	*MAT*α *ade2-1 trp1-1 can1-100 leu2-3,112 his3-11,15 ura3-1 ark1*Δ*::LEU2*
YMC439	*MAT***a** *ade2-1 trp1-1 can1-100 leu2-3,112 his3-11,15 ura3-1 prk1*Δ*::URA3 ark1*Δ*::LEU2*
YMC440	*MAT*α *ade2-1 trp1-1 can1-100 leu2-3,112 his3-11,15 ura3-1 pan1::PAN1-HA-URA3*
YMC441	*MAT***a** *ade2-1 trp1-1 can1-100 leu2-3,112 his3-11,15 ura3-1 pan1::PAN1-Myc-URA3*
YMC442	*MAT***a** *ade2-1 trp1-1 can1-100 leu2-3,112 his3-11,15 ura3-1 prk1*Δ*::URA3 pan1::PAN1-Myc-TRP1*
YMC443	*MAT*α *ade2-1 trp1-1 can1-100 leu2-3,112 his3-11,15 ura3-1 ark1*Δ*::LEU2 pan1::PAN1-Myc-TRP1*
YMC444	*MAT***a** *ade2-1 trp1-1 can1-100 leu2-3,112 his3-11,15 ura3-1 prk1*Δ*::URA3 ark1*Δ*::LEU2 pan1::PAN1-Myc-TRP1*
YMC445	*MAT***a** *ade2-1 trp1-1 can1-100 leu2-3,112 his3-11,15 ura3-1 pan1::PAN-RFP-TRP1 sla1::SLA1-GFP-LEU2*

Immunoprecipitation, Two-Hybrid Assays, and Glutathione S-Transferase (GST) Fusion Protein Binding Experiments

Preparation of yeast extracts, immunoprecipitation, and immunoblotting of the epitope-tagged proteins were performed as described previously (Tang *et al.*, 1997, 2000). Treatment of the immunoprecipitates with calf intestinal phosphatase (CIP) also followed previous procedures (Zeng and Cai, 1999). Yeast extracts to be treated with CIP were prepared with the use of lysis buffer lacking phosphatase inhibitors sodium orthovanadate and *p*-nitrophenylphosphate. The extracts (57 μl) were then incubated with 7 μl of 10× phosphatase buffer and 6 μl of 10 U/μl CIP (Biolabs, Beverly, MA) at 37°C for 40 min before subjected to immunoprecipitation.

For the yeast two-hybrid assay, DNA fragments of *SLA1* and *PRK1* were fused to the HA-tagged *GAL4* activation domain of pGADT7 or the Myc-tagged DNA binding domain of pGBKT7 as indicated in Table 2. Plasmids were cotransformed into the strain SFY526 and the expression of each fusion protein was confirmed by Western blotting with the use of anti-HA or anti-Myc antibodies. The β-galactosidase activities were measured as instructed by the manufacturer (CLONTECH, Palo Alto, CA).

To make GST-fusion proteins, various coding regions of *SLA1*, *PAN1*, and *END3* were obtained by PCR and fused in-frame to a bacterial GST expression vector pGEX-4T-1 (Amersham Pharmacia Biotech, Malaysia) as described in Table 2. Expression and purification of the GST-fusion proteins were performed according to Zeng and Cai (1999), and the GST-fusion protein binding experiments according to Tang *et al.* (2000).

In Vitro Kinase Assays

In vitro kinase assays with the use of GST-fusion proteins as substrates were performed as described (Zeng and Cai, 1999). For Sla1p- and Pan1p-associated kinase assays, the bead-bound anti-

Table 2. Plasmid constructs used in this study

Construct	Description
pGEX-SH3	GST-SH3; the DNA coding region for Sla1p (2-440 a.a.) was generated by PCR and cloned in frame into pGEX-4T-1 (Tang *et al.*, 2000).
pGEX-SR	GST-SR; the DNA coding region for Sla1p (856-1244 a.a.) was generated by PCR and cloned in frame into pGEX-4T-1 (Tang *et al.*, 2000).
pGEX-LR1	GST-LR1; the DNA coding region for Pan 1p (99-383 a.a.) was generated by PCR and cloned in frame into pGEX-4T-1 (Zeng and Cai, 1999).
pGEX-END3	GST-END3; the *END3* coding region was generated by PCR and cloned in frame into pGEX-4T-1 (Zeng and Cai, 1999).
pGBKT7-PRK1^{D158Y}	*PRK1^{D158Y}* coding region was generated by PCR and cloned in frame into pGBKT7.
pGBKT7-PRK1^{D158Y}n	The N-terminal coding region of Prk1^{D158Y}p (1-390 a.a.) in pGBKT7; generated by removing the C-terminal region of *PRK1* from pGBT9-PRK1^{D158Y} with *Spe*I/*Sal*I digestion.
pGBKT7-PRK1c	The DNA coding region for Prk1p (301-810 a.a.) was generated by PCR and cloned in frame into pGBKT7.
pGADT7-SLA1	The DNA coding region for Sla1p (1-1244 a.a.) was generated by PCR and cloned in frame into pGADT7.
pGADT7-SLA1ΔSR	The DNA coding region for Sla1p (1-854 a.a.) was generated by PCR and cloned in frame into pGADT7.
pGADT7-SR	The DNA coding region for Sla1p (856-1244 a.a.) was generated by PCR and cloned in frame into pGADT7.
pGAL-PRK1	*PRK1* coding region was generated by PCR and placed under *GAL1* promoter control in two vectors derived from pRS315 and pRS316, respectively (Zeng and Cai, 1999).
pGAL-PRK1^{D158Y}	*PRK1^{D158Y}* under *GAL1* promoter control in pRS315 and pRS316; generated by replacing the *Sma*I/*Spe*I fragment of pGAL-PRK1 with the *Sma*I/*Spe*I fragment of pPRK1^{D158Y} (Zeng and Cai, 1999).
pGAL-HA-LR1	The DNA coding region for Pan1p (1-385 a.a.) was generated by PCR, cloned in frame with the *HA* epitope, and placed under *GAL1* promoter control in pRS316 (Tang *et al.*, 2000).
pGAL-HA-LR2	The DNA coding region for Pan1p (386-846 a.a.) was generated by PCR, cloned in frame with the *HA* epitope, and placed under *GAL1* promoter control in pRS316 (Tang *et al.*, 2000).
pGAL-HA-SR	The DNA coding region for Sla1p (856-1244 a.a.) was generated by PCR, cloned in frame with the *HA* epitope, and placed under *GAL1* promoter control in pRS316.
pGAL-HA-PRK1	The *PRK1* coding region was generated by PCR, cloned in frame with the *HA* epitope, and placed under *GAL1* promoter control in pRS316 (Zeng and Cai, 1999).
pGAL-HA-PRK1^{D158Y}	*HA-PRK1^{D158Y}* under *GAL1* promoter control in pRS314; generated by replacing the *Sac*I/*Pst*I fragment of pPRK1^{D158Y} with the *Sac*I/*Pst*I fragment of pGAL-HA-PRK1 (Zeng and Cai, 1999).
pRS424-SLA1	*SLA1* gene was generated by PCR and cloned into pRS424 (2μ, *TRP1*).
pMyc-SLA1	The *SLA1* coding region was generated by PCR, cloned in frame with the *Myc* epitope, and placed under its own promoter control in pRS424 and pRS425, respectively.
pPAN1c-HA	The DNA coding region for Pan1p (1252-1480 a.a.) was generated by PCR and cloned in frame with a C-terminal *HA* epitope followed by the *ADH1* terminator in pRS306.
pPAN1c-Myc	The DNA coding region for Pan1p (1252-1480 a.a.) was generated by PCR and cloned in frame with a C-terminal *Myc* epitope followed by the *ADH1* terminator in pRS304 and pRS306, respectively.
pPAN1c-RFP	The DNA coding region for Pan1p (1252-1480 a.a.) was generated by PCR and cloned in frame with a C-terminal *RFP* epitope followed by the *ADH1* terminator in pRS304.
pSLA1c-GFP	The DNA coding region for Sla1p (1105-1244 a.a.) was generated by PCR and cloned in frame with a C-terminal *GFP* epitope followed by the *ADH1* terminator in pRS305.
pYep352-FUR4	*FUR4* gene was generated by PCR and cloned into pYep352 (2μ, *URA3*).

Myc immunoprecipitates were first washed with radioimmunoprecipitation assay buffer (50 mM Tris-HCl [pH 7.2], 1% Triton X-100, 1% sodium deoxycholate, 0.1% SDS, 150 mM NaCl) five times, and another two times with the kinase buffer (25 mM Tris-HCl [pH 7.4], 5 mM β-glycerophosphate, 2 mM dithiothreitol, 0.1 mM sodium orthovanadate, 10 mM $MgCl_2$), followed by suspension in 34.5 μl of the kinase buffer. The kinase assays were performed by incubating the beads with 0.5 μl of [γ-^{32}P]ATP (10 mCi/ml; PerkinElmer Life Sciences, Boston, MA) and 5 μl of 20 μM ATP at 30°C for 40 min and were terminated by 10 μl of 5× loading buffer. The samples were boiled and separated by SDS-PAGE, and proteins were transferred onto a polyvinylidene diflouride membrane (Millipore, Bedford, MA). After overnight exposure to an x-ray film, the membrane was subjected to immunoblotting with the use of anti-Myc antibody.

Gel Filtration Chromatography

Yeast cells were grown with raffinose as the carbon source to the early log phase and galactose was added to a final concentration of 2%. Cells were allowed to grow for another 5 h before being collected. Yeast extracts were prepared with the use of the glass bead lysis method (Dunn and Wobbe, 1993). After polyethylenimine precipitation to remove nucleic acids (Burgess, 1991), the extracts were subjected to ammonium sulfate fractionation. The pellet derived from 60% ammonium sulfate was dissolved in lysis buffer (20 mM Tris-HCl [pH 7.9], 10 mM $MgCl_2$, 1 mM EDTA, 5% glycerol) and dialyzed overnight at 4°C in a large volume of gel filtration buffer (50 mM HEPES [pH 7.3], 150 mM KCl, 0.01% Nonidet P-40). The extracts were then concentrated with the use of polyethylene glycol 8000 and 15 mg of the proteins was loaded onto a SR10/50J column (Amersham Pharmacia Biotech) containing 35 ml of Superose 6 (Amersham Pharmacia Biotech) equilibrated with the gel filtration buffer. Proteins were eluted from the column with the gel filtration buffer at a flow rate of 0.17 ml/min. Ninety fractions were collected in total. Proteins in each fraction were precipitated by 5% of trichloroacetic acid and dissolved in 40 μl of protein loading buffer. Fifteen microliters of these protein samples was then analyzed by SDS-PAGE and immunoblotting.

Cellular Localization of RFP-tagged Pan1p and GFP-tagged Sla1p

Yeast cells were grown to the early log phase at 30°C in raffinose, followed by addition of galactose (to 2%) for 2 h. Cells were then harvested and fixed with formaldehyde (3.7%) for 10 min. After wash with phosphate-buffered saline for three times, cells were suspended in 90% glycerol containing *p*-phenylenediamine and visualized with the fluorescence optics and the Nomarski optics. The images were acquired with the use of a Leica DMAXA microscope equipped with a Hamamatsu C4742-98 digital camera.

Electron Microscopy Analysis

Yeast cultures (1.5 ml) were grown in raffinose to the early log phase followed by addition of galactose to 2% and allowed to grow for another 5 h. Cells were harvested and prefixed with 50% glutaraldehyde solution for 2 h at 25°C. After wash with distilled water three times, cells were fixed in 2% freshly made potassium permanganate for 2 h at 25°C. After several washes with water, cells were dehydrated in a graded series of 50–100% ethanol and embedded in low-viscosity Spurr resin (Sigma, St. Louis, MO). Samples were sectioned, mounted, and stained with uranyl acetate and lead citrate, and viewed under a JEOL 1200EX electron microscope.

Endocytosis Assays

For the lucifer yellow (LY) uptake assay, cells were grown in raffinose to the early log phase at 30°C followed by exposure to 2% galactose for 2 h. LY was added to 5 mg/ml and incubation was continued for another 2 h. Cells were collected and washed five times with phosphate-buffered saline containing 10 mM sodium azide and 50 mM sodium fluoride, followed by suspension in 90% glycerol containing *p*-phenylenediamine and examination with a Zeiss Axioplan microscope.

The uracil permease internalization assay was carried out as described by Volland *et al.* (1994) with minor modifications. Cells containing pRS315, pGAL-PRK1, and pGAL-PRK1^{D158Y} were transformed with pYep352-FUR4 to increase the production of uracil permease. The transformants were grown at 30°C in raffinose to OD_{600} of 0.2–0.3, followed by galactose addition and another 2.5 h of incubation. Cycloheximide was added to 100 μg/ml and samples were taken at 30-min intervals to measure uracil uptake. The uracil uptake assay was performed by incubating 1 ml of the culture with 5 μM [^{14}C]uracil (PerkinElmer Life Sciences) for 20 s at 30°C. The suspension was then quickly filtered through a Whatman GF/C filter, followed by washing twice with ice-old water and counting for the retained radioactivity.

RESULTS

Phosphorylation of Sla1p by Prk1p In Vitro

Previous reports identified Prk1p as a novel serine/threonine kinase regulating the actin cytoskeleton organization in yeast (Cope *et al.*, 1999; Zeng and Cai, 1999). In vitro kinase assays demonstrated that Prk1p could phosphorylate Pan1p specifically on the LxxQxTG motifs (Zeng and Cai, 1999). Pan1p contains multiple LxxQxTG motifs, with five of them found in the first long repeat (LR1) and ten in the second long repeat (LR2) (Sachs and Deardorff, 1992; Zeng and Cai, 1999). Strikingly, another protein from the yeast sequence database that contains multiple LxxQxTG motifs is the Pan1p-interacting protein Sla1p, with five copies of such motif present in its C-terminal region (Figure 1A).

Sla1p is originally identified as a protein required for the viability of the *abp1* mutant and shown to be essential for the proper formation of the cortical actin cytoskeleton (Holtzman *et al.*, 1993). It contains three SH3 domains in the N-terminal region and a repeated motif with a core sequence of TGGAMMP in the C-terminal region (Holtzman *et al.*, 1993). The five copies of the LxxQxTG motif also reside within this region. If a shorter version of the motif, QxTG, is included, the number of the repeats in this region will increase to 14 (Figure 1A). The presence of these motifs in Sla1p suggests that Sla1p may be another substrate of Prk1p.

To test this possibility, the N-terminal SH3 domains and the C-terminal QxTG repeats of Sla1p were expressed as GST fusion proteins (GST-SH3 and GST-SR; Figure 1A) for in vitro kinase assay. As expected, among the three GST-fusion proteins (GST-SR, GST-SH3, and GST itself) tested, only GST-SR could be phosphorylated by the immunoprecipitated HA-Prk1p (Figure 1B, lanes 1–3). The phosphorylation of GST-SR was Prk1p dependent, because no phosphorylation was observed when the immunoprecipitates prepared from cells containing untagged Prk1p were used (Figure 1B, lane 4). In addition, the immunoprecipitates prepared from cells containing an inactive form of Prk1p, Prk1^{D158Y}p (Zeng and Cai, 199), was unable to phosphorylate GST-SR (Figure 1B, lane 5). These results demonstrated that Prk1p could recognize the SR region of Sla1p as an efficient substrate in vitro.

Interaction of Prk1p with Sla1p and Pan1p In Vivo

To obtain additional evidence to prove that Sla1p is a bona fide substrate of Prk1p, we investigated whether Prk1p and Sla1p interact with each other in vivo. Because active kinases interact with their substrates only transiently, the detection of such interactions usually requires the use of mutated forms of the kinases, which are unable to execute the phosphorylation reaction (Han *et al.*, 1997). Indeed, the coimmunoprecipitation experiments with the use of wild-type Prk1p could not ascertain the presence of the Prk1p-Sla1p complex (our unpublished results). However, when HA-Prk1p was replaced by HA-Prk1^{D158Y}p, the Sla1p-Prk1^{D158Y}p complex became readily detectable (Figure 2). As shown in Figure 2A, the anti-Myc immunoprecipitates contained both Myc-Sla1p (Figure 2A, lane 3), and HA-Prk1^{D158Y}p (Figure 2A, lane 5), which could not be precipitated by the anti-Myc antibody when Myc-Sla1p was not present (Figure 2A, lane 4). Therefore, the inactivated Prk1p kinase, Prk1^{D158Y}p, was able to form a stable complex with Sla1p in vivo.

Similar experiments were carried out to test the interaction between Prk1^{D158Y}p and Pan1p. The plasmid pGAL-HA-PRK^{D158Y} was introduced into a strain containing Myc-tagged Pan1p (YMC441). As shown in Figure 2B, HA-Prk1^{D158Y}p was detectable only in the anti-Myc immunoprecipitates made from the cells containing both Myc-Pan1p and HA-Prk1^{D158Y}p (Figure 2B, lane 5), not in that made from cells containing only HA-Prk1^{D158Y}p (Figure 2B, lane 4). This confirmed that Prk1^{D158Y}p also stably associated with Pan1p in vivo.

Next, we sought to determine the approximate regions in Prk1p and Sla1p that are responsible for their association with the use of the two-hybrid protein-protein interaction assay. Pair-wise combinations of constructs containing various coding regions of *prk1^{D158Y}* and *SLA1* were introduced into the strain SFY526 for measurement of the β-galactosidase activity. Western blotting confirmed the expression of these bait and prey proteins to be at similar levels (our unpublished results). As shown in Table 3, the only region

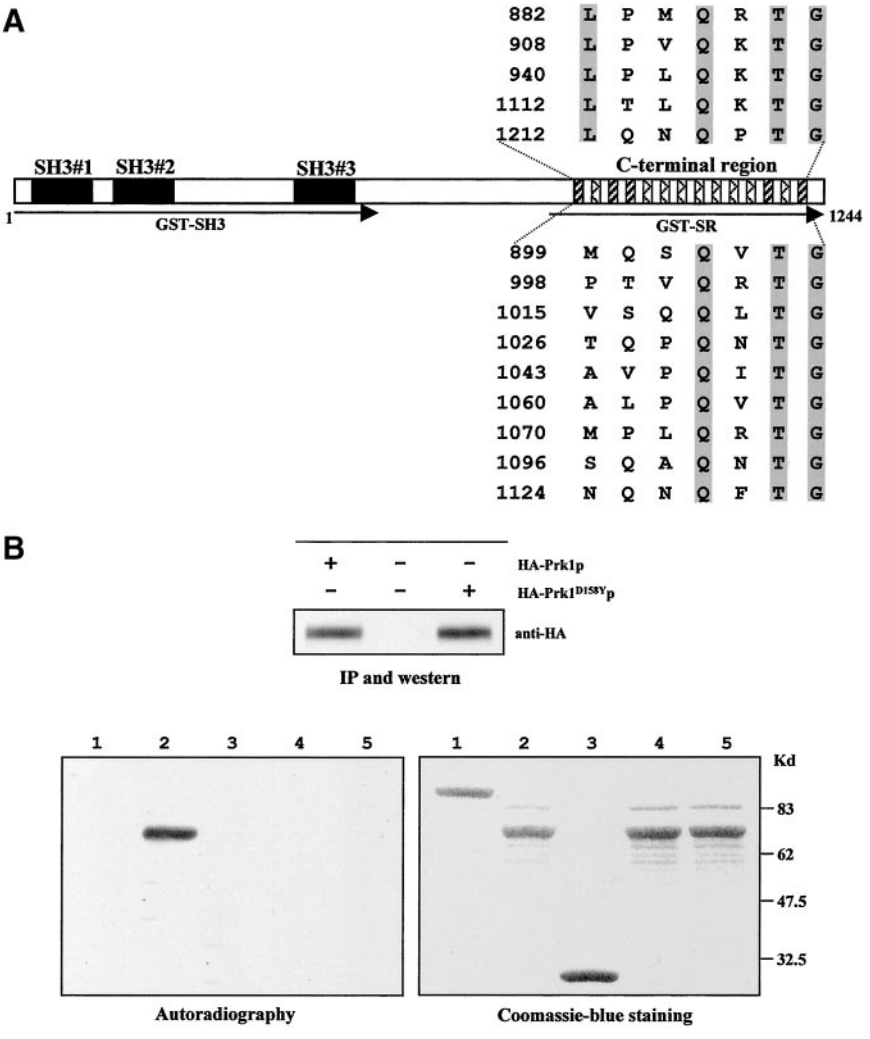

Figure 1. Distribution of the LxxQxTG motif in Sla1p and phosphorylation of Sla1p by Prk1p. (A) Schematic diagram of the protein structure of Sla1p. Sla1p contains three SH3 domains (solid boxes) at the N terminus. The C-terminal region contains five copies of the LxxQxTG motif (black-hatched boxes) and nine copies of the QxTG motif (cross-hatched boxes). The positions of each motif are as shown. The arrows below the diagram indicate the regions of Sla1p used in GST-fusion proteins. (B) In vitro phosphorylation of Sla1p by Prk1p. Wild-type Prk1p and the kinase-inactivated Prk1p (Prk1^{D158Y}p) were expressed as HA-tagged proteins and quantified by immunoprecipitation and Western. Equivalent amounts of the immunoprecipitated proteins were used in the kinase reactions (HA-Prk1p, lane 1–3; HA-Prk1^{D158Y}p, lane 5). Immunoprecipitates from cells containing untagged Prk1p were used in lane 4 as the control. Substrates used in lanes 1–5 were GST-SH3, GST-SR, GST, GST-SR, and GST-SR, respectively. Phosphorylation results were shown as autoradiography (left) and the input substrates were visualized by the Coomassie Blue staining (right).

from Sla1p that exhibited significant interaction with Prk1p was the QxTG rich C-terminal region (856–1244). This region showed much stronger interaction with the Prk1^{D158Y}p kinase domain (1–390) than the full-length Prk1^{D158Y}p. This result further supports that the Prk1p-Sla1p interaction is a kinase-substrate type of interaction.

Phosphorylations of Sla1p and Pan1p by Their Associated Kinases

The finding that blockage of the phosphorylation reaction favored formation of stable Prk1p-Sla1p/Pan1p complexes suggests that the kinase may quickly dissociate from its substrates after phosphorylation is accomplished. Although the transient interactions between wild-type Prk1p and its substrates are difficult to detect by immunoprecipitation and protein blotting, they can still be demonstrated if more sensitive methods are used. One such method is the examination of the Sla1p immunoprecipitates for the Prk1p-dependent kinase activity. A plasmid expressing Myc-tagged Sla1p (pRS424-Myc-SLA1) was introduced into the wild-type strain W303. The anti-Myc immunoprecipitates from the yeast extracts were then directly incubated with [γ-^{32}P]ATP at 30°C for 40 min. After overnight exposure, Myc-Sla1p was found to be phosphorylated by the kinase activities present in the immunoprecipitates (Figure 3A, lane 1). The phosphorylation was specific to Sla1p, because no phosphorylation of any proteins could be seen if Sla1p was not tagged (Figure 3A, lane 2). To prove that Prk1p was the kinase responsible for the phosphorylation, the same experiments were carried out with a *prk1*Δ strain (YMC427). To our surprise, Sla1p immunoprecipitated from the *prk1*Δ mutant could still become phosphorylated after incubating with radioactive ATP (Figure 3A, lane 3). This suggested that either Prk1p was not the underlying kinase, or there could be other kinases present in the complex in addition to Prk1p. The immediate candidate is Ark1p, another kinase that associates with the cortical actin patches. Indeed, when the experiments were carried out with the use of a *prk1*Δ *ark1*Δ strain (YMC439), the anti-Myc immunoprecipitates no longer contained any kinase activities that could phosphor-

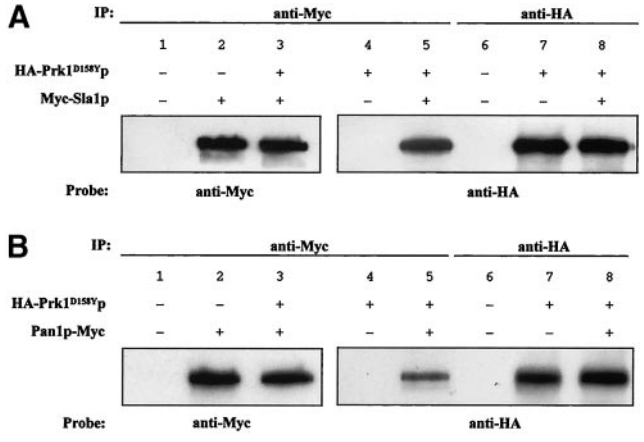

Figure 2. Physical associations of Prk1^{D158Y}p with Sla1p and Pan1p. Yeast extracts prepared from various strains in equal amounts were subjected to anti-Myc or anti-HA immunoprecipitations (IP), gel electrophoresis, and analysis by immunoblotting with the use of anti-Myc and anti-HA antibodies, as indicated. (A) Coimmunoprecipitation of HA-Prk1^{D158Y}p and Myc-Sla1p. Yeast extracts were prepared from the wild-type strain W303 (lanes 1 and 6), W303 containing pGAL-HA-PRK1^{D158Y} (lanes 4 and 7), W303 containing pMyc-SLA1 (lane 2), and W303 containing both pGAL-HA-PRK1^{D158Y} and pMyc-SLA1 (lanes 3, 5, and 8), respectively. (B) Coimmunoprecipitation of HA-Prk1^{D158Y}p and Pan1p-Myc. Yeast extracts were prepared from W303 (lanes 1 and 6), W303 containing pGAL-HA-PRK1^{D158Y} (lanes 4 and 7), YMC441 (*pan1::PAN1-Myc*; lane 2), and YMC441 containing pGAL-HA-PRK1^{D158Y} (lanes 3, 5, and 8), respectively.

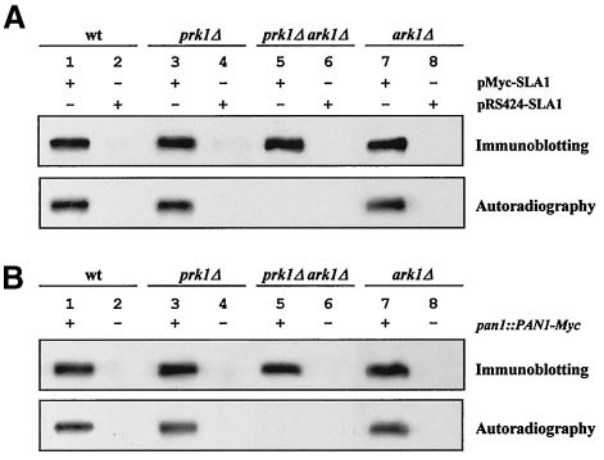

Figure 3. Phosphorylation of Sla1p and Pan1p by their associated kinases. Equal amounts of yeast extracts prepared from various strains were subjected to anti-Myc immunoprecipitation followed by kinase reaction as described in MATERIALS AND METHODS. The samples were electrophoresed and analyzed by autoradiography and immunoblotting. (A) Phosphorylation of Sla1p. Yeast extracts were prepared from W303 (wt, lanes 1 and 2), YMC427 (*prk1*Δ, lanes 3 and 4), YMC439 (*prk1*Δ *ark1*Δ, lanes 5 and 6), and YMC438 (*ark1*Δ, lanes 7 and 8) containing either pMyc-SLA1 (lanes 1, 3, 5, and 7) or pRS424-SLA1 (lanes 2, 4, 6, and 8), respectively. (B) Phosphorylation of Pan1p. Yeast extracts were prepared from YMC441 (*pan1::PAN1-Myc*; lane 1), W303 (lane 2), YMC442 (*prk1*Δ *pan1::PAN1-Myc*; lane 3), YMC427 (*prk1*Δ; lane 4), YMC444 (*prk1*Δ *ark1*Δ *pan1::PAN1-Myc*; lane 5), YMC439 (*prk1*Δ *ark1*Δ; lane 6), YMC443 (*ark1*Δ *pan1::PAN1-Myc*; lane 7), and YMC438 (*ark1*Δ; lane 8), respectively.

ylate Sla1p (Figure 3A, lane 5). Deletion of the *ARK1* gene alone (*ark1*Δ, YMC438) was not sufficient to abolish the kinase activity (Figure 3A, lane 7). It is concluded, therefore, that Sla1p associates with two kinases in vivo, Prk1p and Ark1p, either at the same time or separately.

Similarly, phosphorylation of the immunoprecipitated Myc-Pan1p could be observed in the wild-type strain (Figure 3B, lane 1), the *prk1* single mutant (Figure 3B, lane 3), and the *ark1* single mutant (Figure 3B, lane 7), but not in the *prk1 ark1* double mutant (Figure 3B, lane 5), following the same pattern of Sla1p.

Obstruction of Sla1p/Pan1p Interaction by Prk1p-dependent Phosphorylation

One possible purpose for Prk1p to phosphorylate Sla1p and Pan1p is to regulate the physical interaction between Sla1p and Pan1p, because the regions that contain the Prk1p phosphorylation sites in the two proteins, the Sla1 repeats (SR) in the C-terminal region of Sla1p and the LR1 in the N-terminal region of Pan1p, are also the regions required for the interaction between them (Tang *et al.*, 2000). This possibility was tested by the following experiments. First, the effect of phosphorylation of LR1 on its interaction with GST-fused SR was

Table 3. Two-hybrid interactions between Prk1p and Sla1p proteins

Units of β-galactosidase activity were determined in SFY526 cells transformed with the indicated pair of plasmids as described in MATERIALS AND METHODS.

	Prey			
Bait	pGADT7 (vector)	Sla1p (1-1244 a.a.)	Sla1p (1-854 a.a.)	Sla1p (856-1244 a.a.)
pGBKT7 (vector)	<0.50	<0.50	<0.50	<0.50
Prk1^{D158Y}p (1-810 a.a.)	<0.50	3.22 ± 0.11	<0.50	7.25 ± 0.27
Prk1^{D158Y}p (1-390 a.a.)	<0.50	33.35 ± 1.31	<0.50	47.79 ± 3.97
Prk1p (301-810 a.a.)	<0.50	<0.50	<0.50	<0.50
		(units of β-galactosidase activity)		

examined. As shown in Figure 4, HA-LR1 immunoprecipitated from wild-type cells migrated as a single band (Figure 4A, lane 2). However, when this protein was immunoprecipitated from cells overexpressing *PRK1,* it migrated with a slower mobility with the band becoming broader and smeared (Figure 4A, lane 4). The protein mobility shift was confirmed to be due to phosphorylation, because a treatment by CIP before electrophoresis reversed this phenomenon (Figure 4A, lane 5). Treatment of the cell extracts by phosphatase before the immunoprecipitation also achieved same result (Figure 4A, lane 6). The mobility shift of HA-LR1 was not observed in cells overexpressing the inactive Prk1p kinase (Figure 4A, lane 3), indicating that it was the elevated Prk1p kinase activity that was responsible for the mobility change. The mobility shift of HA-LR1 as a result of Prk1p overproduction provided a convenient means for testing its ability to bind the GST-fused SR. Various yeast extracts were first incubated with equal amounts of immobilized GST-SR. After binding and washing, the bound proteins were separated by SDS-PAGE and probed with the anti-HA antibody. As reported previously (Tang *et al.*, 2000), the HA-LR1 protein in wild-type cells could be precipitated readily by GST-SR (Figure 4B, lane 2). In contrast, GST-SR could only precipitate down a minute amount of HA-LR1 in *PRK1*-overexpressing cells (Figure 4B, lane 4), suggesting that the hyperphosphorylated HA-LR1 was incompetent in interacting with GST-SR. A strong interaction could be restored after dephosphorylation of HA-LR1 by CIP treatment (Figure 4B, lane 5). These results demonstrated that the ability of Pan1p to interact with Sla1p was impaired by the Prk1p-dependent phosphorylation.

A reciprocal experiment was then carried out to test whether phosphorylation of the Sla1 repeats could affect its binding to Pan1p. To obtain the hyperphosphorylated form of SR, the plasmid pGAL-HA-SR was introduced together with pGAL-PRK1 into wild-type cells. Like HA-LR1 in the above-mentioned experiment, HA-SR from wild-type cells appeared as a single band in SDS-PAGE (Figure 4C, lanes 2 and 3), whereas it migrated as a higher and broader band with a smeared tail after experiencing the *PRK1* overexpression (Figure 4C, lane 4). Again, phosphatase treatment confirmed that this mobility shift of SR was due to phosphorylation (Figure 4C, lane 5). The GST-fusion protein binding assay essentially replicated the findings obtained with the use of HA-LR1, i.e., HA-SR from cells containing no overexpressed *PRK1* could be precipitated by GST-LR1 (Figure 4D, lanes 2 and 4), whereas its binding to GST-LR1 was almost undetectable after it was hyperphosphorylated (Figure 4D, lane 3).

The results of GST-fusion protein binding assays were further strengthened by the data obtained from the gel filtration experiments. When yeast extracts were prepared from wild-type cells and fractionated by gel filtration on a Superose 6 column, Sla1p was found to be coeluted with Pan1p. Both proteins were eluted with the peak position corresponding to a molecular mass of 700 kDa (Figure 5A). In contrast, when yeast extracts prepared from cells overexpressing *PRK1* were subjected to the same protocol, Sla1p appeared in much later fractions (corresponding to a molecular mass of 150 kDa), which were distinct from the fractions containing the majority of Pan1p (Figure 5B). In a control experiment with the use of cells overexpressing *prk1^{D158Y}*,

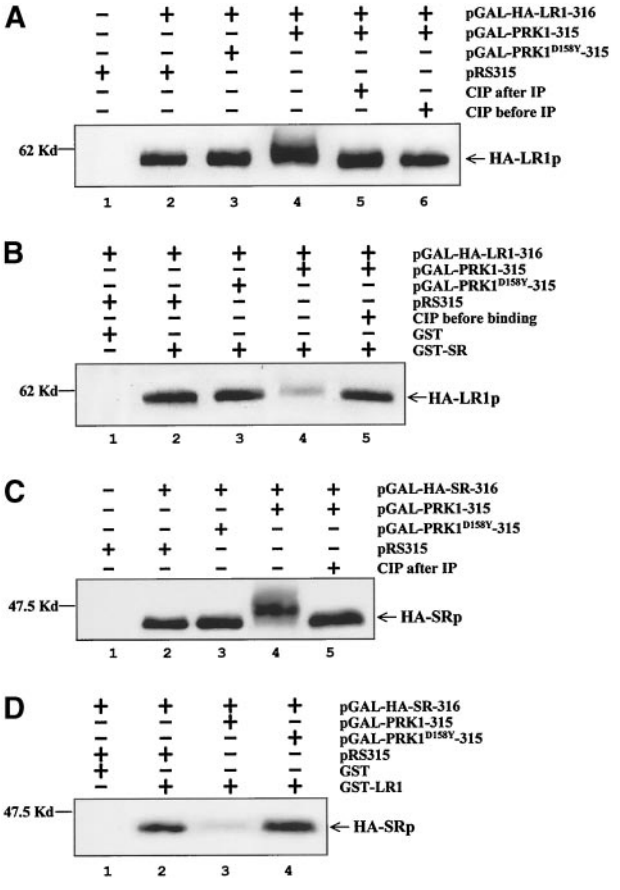

Figure 4. Hindrance of the Pan1p/Sla1p interaction by Prk1p-dependent phosphorylation. (A) Phosphorylation of LR1 by Prk1p in vivo. Yeast extracts in equal amounts prepared from W303 containing pRS316 and pRS315 (lane 1), pGAL-HA-LR1 and pRS315 (lane 2), pGAL-HA-LR1 and pGAL-PRK1^{D158Y} (lane 3), and pGAL-HA-LR1 and pGAL-PRK1 (lanes 4, 5, and 6) were subjected to anti-HA immunoprecipitation and immunoblotting. In lane 5, the immunoprecipitates were treated with CIP before electrophoresis. In lane 6, the yeast extracts were incubated with CIP before immunoprecipitation. (B) Binding of HA-LR1 to GST-SR. Yeast extracts in the same amounts as used for anti-HA immunoprecipitation prepared from W303 containing pGAL-HA-LR1 and pRS315 (lanes 1 and 2), pGAL-HA-LR1 and pGAL-PRK1^{D158Y} (lane 3), and pGAL-HA-LR1 and pGAL-PRK1 (lanes 4 and 5) were incubated with immobilized GST (lane 1), and GST-SR (lanes 2–5), respectively. The precipitates were separated by SDS-PAGE and immunoblotted with anti-HA antibody. In lane 5, the yeast extracts were treated with CIP before incubation with GST-SR. (C) Phosphorylation of SR by Prk1p in vivo. Equal amounts of yeast extracts prepared from W303 containing pRS316 and pRS315 (lane 1), pGAL-HA-SR and pRS315 (lane 2), pGAL-HA-SR and pGAL-PRK1^{D158Y} (lane 3), and pGAL-HA-SR and pGAL-PRK1 (lanes 4 and 5) were subjected to anti-HA immunoprecipitation and immunoblotting. In lane 5, the immunoprecipitates were treated with CIP before electrophoresis. HA-SR in the yeast extracts treated with CIP before IP was not presented because it got mostly degraded after the treatment. (D) Binding of HA-SR to GST-LR1. Yeast extracts in the same amounts as used for anti-HA immunoprecipitation prepared from W303 containing pGAL-HA-SR and pRS315 (lanes 1 and 2), pGAL-HA-SR and pGAL-PRK1 (lane 3), and pGAL-HA-SR and pGAL-PRK1^{D158Y} (lane 4) were incubated with immobilized GST (lane 1) and GST-LR1 (lanes 2–4), respectively. The precipitates were separated by SDS-PAGE and immunoblotted with anti-HA antibody.

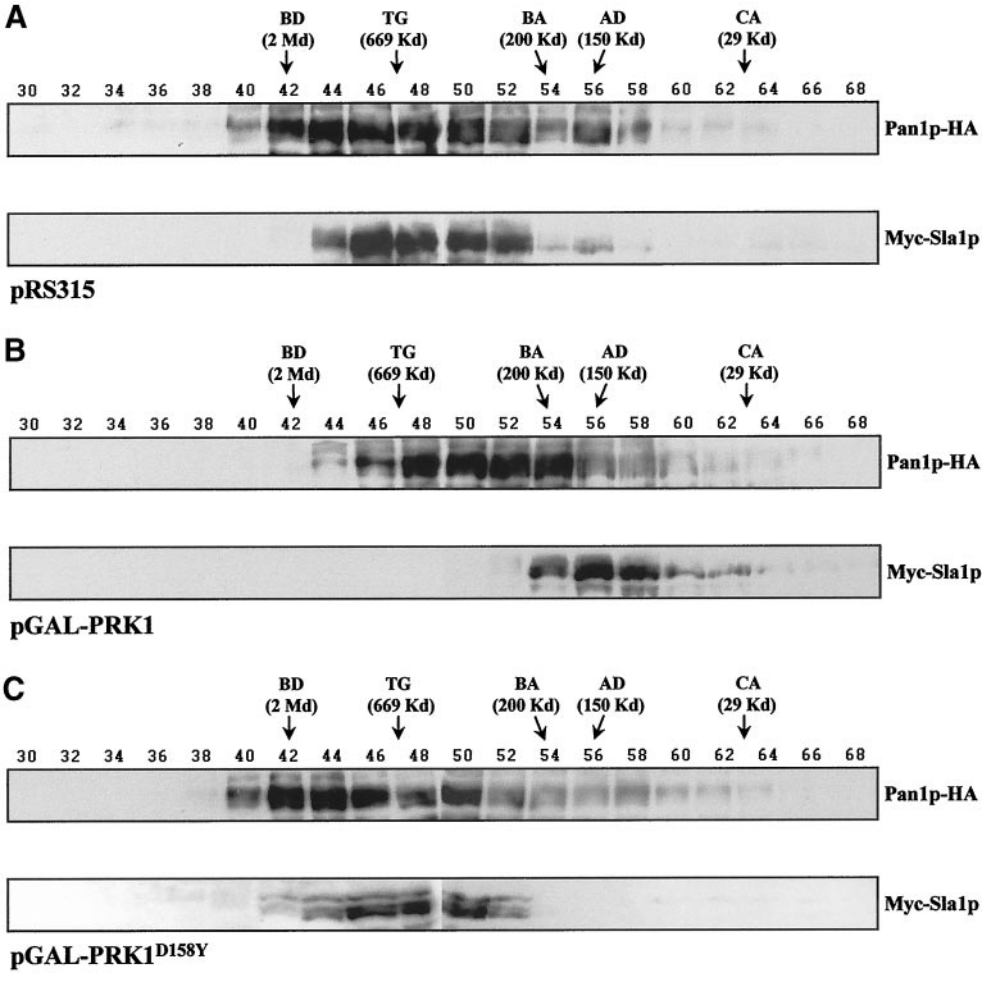

Figure 5. Dissociation of Pan1p and Sla1p in *PRK1* overexpressing Cells. Yeast extracts prepared from YMC440 (*pan1::PAN1-HA*) containing pMyc-SLA1 and pRS315 (A), pMyc-SLA1 and pGAL-PRK1 (B), and pMyc-SLA1 and pGAL-PRK1^{D158Y} (C), were fractionated by gel filtration on a Superose 6 column as described in MATERIALS AND METHODS. Fractions were examined for the presence of Pan1p-HA and Myc-Sla1p. The column was precalibrated with the molecular mass markers as indicated. BD, blue dextran; TG, thyroglobulin; BA, β-amylase; AD, alcohol dehydrogenase; CA, carbonic anhydrase.

the elution pattern of Sla1p and Pan1p was unchanged (Figure 5C). Taken together, these results show that elevation of the Prk1p kinase activity leads to a disintegration of the Sla1p/Pan1p complex, in agreement with the model that Prk1p negatively regulates the function of the Pan1p/Sla1p complex by affecting the interaction between them.

Disruption of Cellular Colocalization of Sla1p and Pan1p by Elevated Prk1p Activity

Although Sla1p and Pan1p have been shown to interact with each other by various methods, their cellular localization patterns have not been directly compared. Therefore, fluorescent protein labeling was used to see whether the two proteins indeed colocalize with each other. A yeast strain (YMC445) containing green fluorescent protein (GFP)-tagged Sla1p and red fluorescent protein (RFP)-tagged Pan1p expressed from their native promoters was created as described in MATERIALS AND METHODS. This strain was indistinguishable from the wild-type in growth rate and the actin cytoskeleton organization (our unpublished results). When visualized under fluorescent microscope, both Pan1-RFP and Sla1-GFP existed as punctate structures with a pattern of cell cycle distribution characteristic of the cortical actin patches (Figure 6A). As expected, Pan1-RFP and Sla1-GFP were found to colocalize well with each other, either as dispersed patches, or in the polarized states such as at the presumptive bud site in unbudded cells and at the mother-bud junction in large-budded cells (Figure 6A).

Given the findings that overexpression of *PRK1* impaired the interaction between Sla1p and Pan1p, it is likely that *PRK1* overexpression will affect their cellular colocalization. To investigate this possibility, the pGAL-PRK1 plasmid was introduced into the strain YMC445. Before induction of *PRK1* by galactose, the cells showed a clear colocalization between Pan1-RFP and Sla1-GFP (Figure 6B, top). After 2 h of induction by galactose, however, >30% of the cells had lost the punctate Sla1-GFP structures, whereas the distribution of Pan1-RFP was essentially undisturbed (Figure 6B, bottom). The change in Sla1-GFP distribution was not due to the addition of galactose per se, because galactose did not have any effect on the colocalization between Sla1-GFP and Pan1-RFP in the cells containing either the control plasmid pRS316 (Figure 6A, bottom), or the inactivated kinase *prk1^{D158Y}* similarly expressed by the *GAL1* promoter (Figure 6C bottom). These results are again in support of the con-

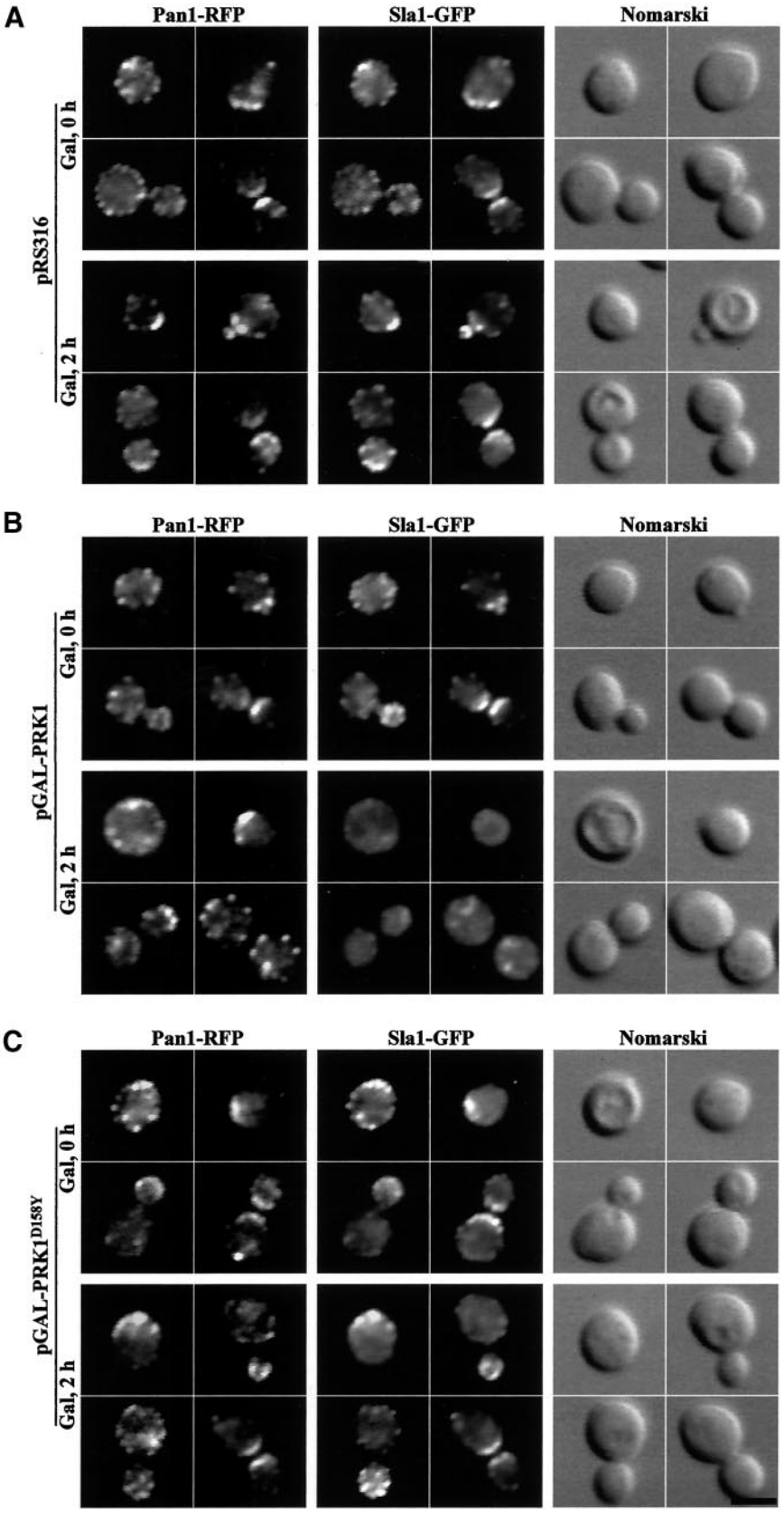

Figure 6. Disruption of the colocalization of Pan1p and Sla1p by *PRK1* overexpression. YMC445 (*pan1::PAN1-RFP sla1::SLA1-GFP*) containing pRS316 (A), pGAL-PRK1 (B), and pGAL-PRK1^{D158Y} (C) were grown to the log phase in medium without galactose (Gal, 0 h) or with galactose (Gal, 2 h). Cells were fixed and visualized for Pan1-RFP (left), Sla1-GFP (middle), and Nomarski image (right) by Leica DMRXA microscope. Bar, 5 μm.

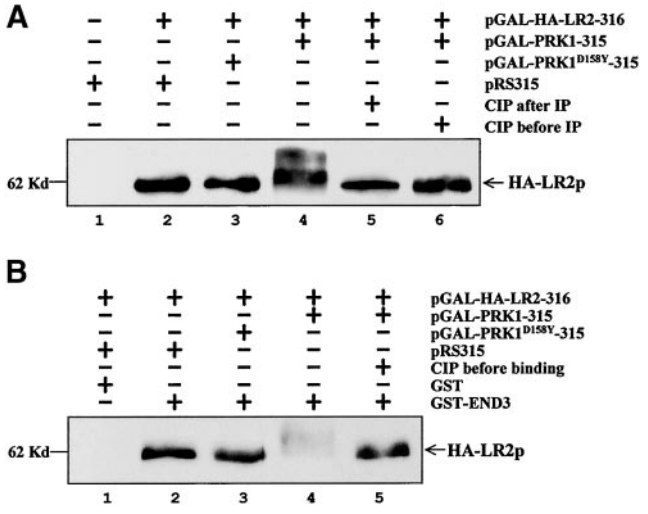

Figure 7. Hindrance of the Pan1p/End3p interaction by Prk1p-dependent phosphorylation. (A) Phosphorylation of LR2 by Prk1p in vivo. Yeast extracts in equal amounts prepared from W303 containing pRS316 and pRS315 (lane 1), pGAL-HA-LR2 and pRS315 (lane 2), pGAL-HA-LR2 and pGAL-PRK1^{D158Y} (lane 3), and pGAL-HA-LR2 and pGAL-PRK1 (lanes 4, 5, and 6) were subjected to anti-HA immunoprecipitation and immunoblotting. In lane 5, the immunoprecipitates were treated with CIP before electrophoresis. In lane 6, the yeast extracts were incubated with CIP before immunoprecipitation. (B) Binding of HA-LR2 to GST-END3. Yeast extracts in the same amounts as used for anti-HA immunoprecipitation prepared from W303 containing pGAL-HA-LR2 and pRS315 (lanes 1 and 2), pGAL-HA-LR1 and pGAL-PRK1^{D158Y} (lane 3), and pGAL-HA-LR1 and pGAL-PRK1 (lanes 4 and 5) were incubated with immobilized GST (lane 1) and GST-END3 (lanes 2–5), respectively. The precipitates were separated by SDS-PAGE and immunoblotted with anti-HA antibody. In lane 5, the yeast extracts were treated with CIP before incubation with GST-SR.

clusion that the association of Sla1p and Pan1p in vivo was disrupted by elevated Prk1 kinase activity.

Obstruction of Pan1p/End3p Interaction by Prk1p-dependent Phosphorylation

It has been shown previously that Pan1p interacts with Sla1p through its LR1 region and interacts with End3p through its LR2 region to form a trimeric complex in vivo (Tang *et al.*, 2000). Similar to LR1, LR2 is also rich in Prk1p phosphorylation sites, the LxxQxTG repeats. In vitro experiments have shown that the presence of excess End3p antagonized the Prk1p phosphorylation of LR2 (Zeng and Cai, 1999). It is therefore possible that Prk1p phosphorylation may also inhibit the interaction between Pan1p and End3p. This possibility was tested by the GST-fusion protein binding assay. An HA-tagged LR2 construct (HA-LR2) was generated to comprise the region that has been shown to interact with End3p in the two-hybrid assay (Tang *et al.*, 1997). Although HA-LR2 immunoprecipitated from wild-type cells migrated as a single band (Figure 7A, lane 2), it appeared as multiple bands with slower mobilities when immunoprecipitated from cells overexpressing *PRK1* (Figure 7A, lane 4). The mobility shift was confirmed by phosphatase treatment to be due to phosphorylation (Figure 7A, lanes 5 and 6). Overproduction of the inactive Prk1p, Prk1^{D158Y}p, had no effect on the mobility of HA-LR2 (Figure 7A, lane 3). When the binding assays were carried out with the use of GST-END3, the results were similar to the LR1 and GST-SR experiment presented in Figure 4. Only the unphosphorylated HA-LR2 could be efficiently precipitated by GST-END3 (Figure 7B, lanes 2 and 3). The hyperphosphorylated HA-LR2 was essentially inert in interacting with GST-END3 (Figure 7B, lane 4). On dephosphorylation by CIP treatment before binding, HA-LR2 from *PRK1*-overexpressing cells regained its ability to interact with GST-END3 (Figure 7B, lane 5). Therefore, similarly to the Pan1p/Sla1p interaction, the Pan1p/End3p interaction is also hindered by Prk1p overproduction. These results again support the hypothesis that Prk1p negatively regulates the complex formation between Pan1p, Sla1p, and End3p proteins.

Endocytosis Defects as a Result of PRK1 Overexpression

The Pan1p/Sla1p/End3p complex is required for multiple cellular functions, including cortical actin organization, endocytosis, and cell wall morphogenesis (Tang *et al.*, 2000). If Prk1p negatively regulates the complex formation between these proteins, it is expected that *PRK1* overexpression in wild-type cells will lead to the defects in these functions similar to those identified in each of the *pan1*, *sla1*, and *end3* mutants. The defective actin cytoskeleton organization similar to that in the *pan1-4* mutant as a result of *PRK1* overexpression has already been reported (Zeng and Cai, 1999). Here we describe the endocytosis defects caused by *PRK1* overexpression.

First, we examined the effect of *PRK1* overexpression on fluid-phase endocytosis with the use of the LY uptake assay (Dulic *et al.*, 1991). To minimize the lethal effect of *PRK1* overexpression (Zeng and Cai, 1999), the exposure of pGAL-PRK1-containing cells to galactose was limited to 2 h, followed by another 2 h of incubation with LY in the presence of galactose. Although most of the cells containing the control plasmid pRS315 were able to internalize LY and exhibited an unambiguous vacuolar staining (Figure 8A, left), only a small portion (<10%) of the cells containing the pGAL-PRK1 plasmid showed clear vacuolar staining (Figure 8A, middle). Moreover, ~20% of these cells were seen to be brightly and uniformly stained, due probably to cell lysis. A similar observation has also been made for the *pan1-4* mutant (Tang *et al.*, 1997). On the other hand, the cells overexpressing the inactive Prk1p, *prk1^{D158Y}*, accumulated LY in the vacuoles normally (Figure 8A, right). These results suggest that the fluid-phase endocytosis was impaired in the Prk1p-overproducing cells.

Next, we examined the effects of *PRK1* overexpression on the internalization step of membrane protein endocytosis by the uracil permease internalization assay (Volland *et al.*, 1994). The yeast plasma membrane protein uracil permease, encoded by *FUR4*, is internalized by endocytosis and degraded in the vacuole under adverse conditions such as inhibition of protein synthesis by cycloheximide (Volland *et al.*, 1994). The diminishing uracil uptake activity from the cell surface, therefore, can be used as a measurement for the internalization step of endocytosis. As shown in Figure 8B, upon the addition of cycloheximide, cells containing the

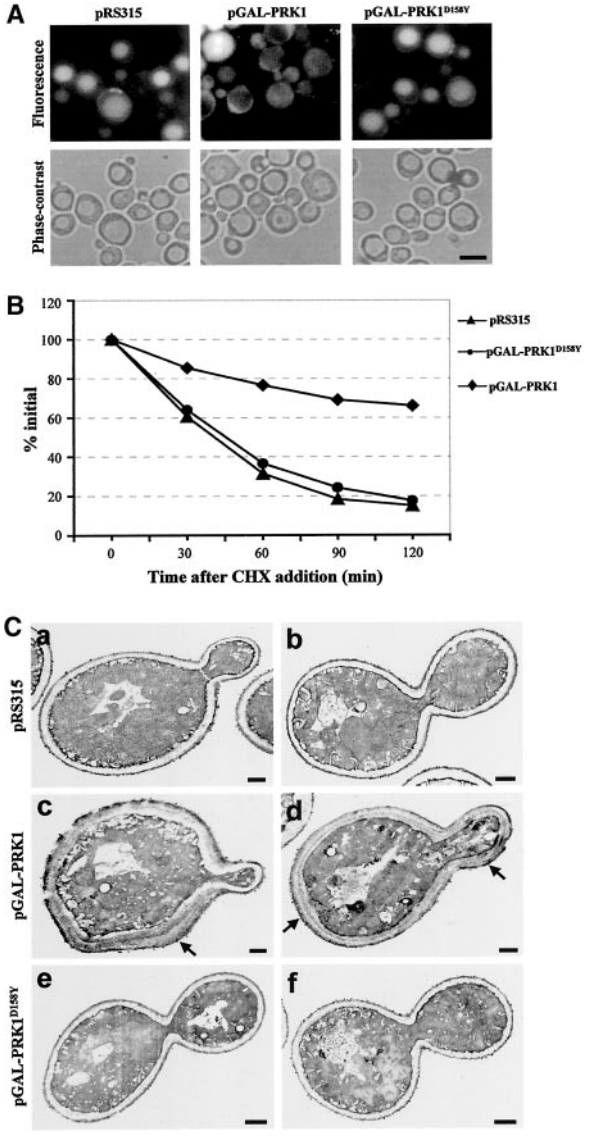

Figure 8. Phenotypic analysis of cells overexpressing *PRK1*. (A) LY accumulation in wild-type strain W303 containing pRS315 (left), pGAL-PRK1 (middle), and pGAL-PRK1^{D158Y} (right). Cells were incubated with LY at 30°C for 2 h and visualized with fluorescein isothiocyanate fluorescence optics (top) and phase-contrast optics (bottom). Bar, 5 μm. (B) Internalization of uracil permease in W303 containing pRS315 (▲), pGAL-PRK1 (♦), and pGAL-PRK1^{D158Y} (●). The uracil permease assays were performed as described in MATERIALS AND METHODS. On addition of cycloheximide (CHX), uracil permease levels at the cell surface decreased. Transport of [^{14}C]uracil into yeast cells was used as a measurement for the relative amounts of uracil permease retained on the cell surface. Uracil uptake is plotted as the percentage activity relative to the initial time point. The results shown are the averages of two independent assays. (C) Cell wall morphology of W303 containing pRS315 (a and b), pGAL-PRK1 (c and d), and pGAL-PRK1^{D158Y} (e and f). After exposure to galactose for 5 h, cells were prefixed and processed for electron microscopy with the use of potassium permanganate fixation to enhance visualization of the cell wall and membranes. The arrows in panels c and d indicate the aberrant cell walls which are thicker and consist of more than one layer. Bars, 500 nm.

control plasmid pRS315 internalized the uracil permease quickly, resulting in a rapid decrease in uracil uptake. However, the cells overexpressing *PRK1* maintained a high activity for uracil uptake under the same conditions. Two hours after the addition of cycloheximide, for example, at least 60% of the uracil uptake activity was still observed in cells overexpressing *PRK1*, whereas ≤20% of such activity was retained in the control cells. Again, overexpression of *prk1^{D158Y}* imposed no effect on the rate of the uracil permease internalization (Figure 8B). These data suggest that elevated Prk1 kinase activity leads to a defect in the process of membrane protein endocytosis at the internalization step.

Cell Wall Defects Caused by PRK1 Overexpression

Cell wall abnormalities are another common phenotype exhibited by the *pan1*, *sla1*, and *end3* mutants (Ayscough *et al.*, 1999; Tang *et al.*, 2000). We next determined whether this defect could also be manifested through *PRK1* overexpression. Cells containing pGAL-PRK1 or the control plasmids were grown to the early log phase and exposed to galactose for 5 h. They were then treated with glutaraldehyde and processed for electron microscopy with the use of the potassium permanganate fixation method. As shown in Figure 8C, cells containing the control plasmid pRS315 displayed a normal cell wall morphology. They had a single layer of cell wall with no apparent difference between the mother and the bud (Figure 8C, a and b). In contrast, ~40% of the cells containing pGAL-PRK1 exhibited aberrant cell wall morphologies similar to what had been observed in the *pan1*, *sla1*, and *end3* mutants (Ayscough *et al.*, 1999; Tang *et al.*, 2000). These included thickened and multilayered cell wall frequently seen to be restricted to the mother cell (Figure 8C, c), although occasionally some daughter cells showed such cell wall abnormalities as well (Figure 8C, d). As a control, cells overproducing inactive Prk1p, Prk1^{D158Y}p, displayed a normal cell wall morphology (Figure 8C, e and f). These results agree with the suggestion that elevated Prk1 kinase activity leads to the disintegration of the Pan1p/Sla1p/End3p complex thereby causing various defects commonly observed in the *pan1*, *sla1*, and *end3* mutants.

DISCUSSION

Identification of Sla1p as a New Substrate of Prk1p

It is remarkable that the two cortical actin patch regulatory proteins, Sla1p and Pan1p, are the only two yeast proteins that contain multiple LxxQxTG motifs that have been identified as the Prk1p phosphorylation sites in vitro. It is therefore anticipated that Sla1p may be another substrate for Prk1p. The evidence to support Sla1p as a bona fide phosphorylation target of Prk1p includes that Sla1p could be phosphorylated by Prk1p in vitro and that Sla1p, as well as Pan1p, were found to be physically associated with Prk1p in vivo. The detection by coimmunoprecipitation was greatly enhanced with the use of the catalytic site mutated Prk1p, indicating that the association between the wild-type kinase and Sla1p/Pan1p is transient and the dissociation occurs quickly after the phosphorylation reaction is accomplished. This notion is certainly in line with the finding that it was the C-terminal region of Sla1p that was responsible for interacting with the kinase domain of Prk1^{D158Y}p. It is therefore not

surprising that Sla1p (and Pan1p) immunoprecipitated from wild-type cells contained only a small quantity of kinase activities. Even though these residual kinase molecules coimmunoprecipitated with Sla1p or Pan1p were beyond the detection by antibody probing, they could still be uncovered by the highly sensitive method of radioactive labeling. With the use of the cell extracts prepared from various mutants, these kinase activities were identified as Prk1p and Ark1p dependent.

The finding that the Sla1p (and Pan1p) immunoprecipitates possessed *PRK1*- and *ARK1*-dependent kinase activities is particularly interesting. Ark1p is first identified as a Sla2p-binding protein from a two-hybrid screen (Cope *et al.*, 1999). It shares extensive sequence homology with Prk1p and is similarly localized to the cortical actin patches (Cope *et al.*, 1999). Although Ark1p contains a kinase domain that is 70% identical to that of Prk1p, its kinase activity has not been experimentally demonstrated either in vivo or in vitro. Our experiments provided the direct evidence for the previous suggestion that these two kinases may perform some overlapping functions in regulating the actin patches (Cope *et al.*, 1999). The association of both Prk1p and Ark1p with Pan1p/Sla1p suggest that either the two kinases regulate Pan1p/Sla1p separately, each representing a distinct signaling pathway to control the actin patch function in response to different cues, or they are functionally redundant as far as the regulation of Pan1p and Sla1p is concerned.

Inhibition of Pan1p/Sla1p/End3p Complex Formation by Prk1p

The interaction between Sla1p and Pan1p involves the C-terminal region of Sla1p and the first long repeat of Pan1p (Tang *et al.*, 2000), both of which contain multiple Prk1p phosphorylation sites. It is therefore evident that this interaction may be regulated by Prk1p phosphorylation. Regulation of protein interactions by kinase phosphorylation is a common phenomenon in signaling pathways. For example, the interaction between Sos1 and Grb2 in human cells is regulated by the mitogen-activated protein kinase (Corbalan-Garcia *et al.*, 1996). Similarly, the autophosphorylation of human p21 activated kinase blocks the binding by Nck or PIX (Zhao *et al.*, 2000). The regulation of the interaction between Pan1p and Sla1p by Prk1p was demonstrated with the use of several approaches. First, the GST-fusion protein binding assay clearly showed that phosphorylation on HA-LR1 and HA-SR greatly hindered the bindings to their GST-tagged interacting partners. The interaction between HA-LR2 and GST-End3p was also inhibited by Prk1p-dependent phosphorylation. Second, with the use of our gel filtration protocols, Pan1p and Sla1p were observed to migrate together at ~700 K_d in wild-type cells, whereas they emerged separately with smaller molecular masses in the presence of elevated Prk1p kinase activity. Third, it was shown that Sla1p and Pan1p no longer colocalized with each other in cells overexpressing *PRK1*. The fact that Sla1p lost the punctate structures while the Pan1p localization remained largely unchanged in the *PRK1* overexpression cells implies that Pan1p and Sla1p acquire the patch localization through different means. The Prk1p-induced disappearance of the Sla1-GFP signal from the cortical patches was unlikely due to a marked degradation of Sla1p, because the protein was still readily detectable in the *PRK1* overexpression cells (Figure 5B).

Although it is always possible that hyperphosphorylation of a given target protein in the presence of an overproduced kinase could be caused by a secondary phosphorylation event, we tend to believe that the above-mentioned results are attributed to the direct phosphorylation of Pan1p and Sla1p by Prk1p for the simple reason that the Pan1p and Sla1p sequences that became hyperphosphorylated under these conditions are rich in LxxQxTG motifs. Therefore, these results in our view constitute compelling evidence to support the model that the complex formation between Pan1p, Sla1p, and End3p proteins are negatively regulated by Prk1p phosphorylation.

Physiological Consequences of PRK1 Overexpression

Pan1p, Sla1p, and End3p are components of a complex that plays important roles in actin patch functions and organization, endocytosis, and cell wall morphogenesis (Tang *et al.*, 2000). Mutations in each of the three genes resulted in essentially identical phenotypes in these processes (Holtzman *et al.*, 1993; Bénédetti *et al.*, 1994; Tang and Cai, 1996; Tang *et al.*, 1997, 2000; Ayscough *et al.*, 1999). To procure functional evidence for the regulation of complex formation between Pan1p, Sla1p, and End3p by Prk1p, the phenotypes of Prk1p overproduction were investigated. It is shown here that overexpression of *PRK1* also leads to cell wall defects similar to those observed in the *pan1*, *sla1*, and *end3* mutants. There is, nevertheless, a minor difference in these aberrant cell wall morphologies between the mutants and the *PRK1*-overexpressing cells. Although the thickened cell walls in the mutant rarely extend beyond the mother cell, this seemed to occur more often in the *PRK1*-overexpressing cells. The significance of this small difference has not been explored. The *PRK1*-overexpressing cells also exhibited defects in fluid phase endocytosis and the internalization of the membrane protein uracil permease. The *prk1*Δ mutant, on the other hand, was normal in both processes (our unpublished results). These findings are in agreement with the negative role of Prk1p in regulating the function of the Pan1p/Sla1p/End3p complex.

Even though the phenotypes resulted from *PRK1* overexpression support the model of negative regulation of the Pan1p/Sla1p/End3p functions, exactly when and how the regulation takes place in a living cell are unknown. It has been noticed previously that, in most of the *prk1* mutant cells at 37°C, the actin patches were not maintained in a polarized manner, and bud emergence and bud growth were also significantly delayed (Zeng and Cai, 1999). This phenotype is indicative of a role for Prk1p in the polarization of the actin patches at G1/S transition. However, whether it is related to the regulation of the Pan1p/Sla1p/End3p complex remains to be investigated.

Diverse Functions of Sla1p

An important piece of evidence concerning the regulation of Pan1p by Prk1p was the suppression of the *pan1-4* mutant by *prk1*Δ (Zeng and Cai, 1999). *prk1*Δ also suppressed the *end3*Δ mutant (Zeng and Cai, 1999). In the light of the new finding that Sla1p is another substrate of Prk1p, it may be speculated that loss of Prk1p activity may also confer sup-

pression to the *sla1* mutant. This, however, was not the case. *prk1*Δ could not suppress the temperature sensitivity of the *sla1* null mutant (our unpublished results). This result raises the possibility that Sla1p may also be involved in functions distinct from that of the Pan1p/Sla1p/End3p complex. The suppression of *pan1-4* by *prk1*Δ requires the presence of the mutant Pan1p, and hence is a result of rejuvenation of the mutant Pan1p protein rather than a bypass of the Pan1p function (Zeng and Cai, 1999). *pan1-4* is a nonsense mutation near the end of the LR2, generating a truncated protein that has retained all the Prk1p phosphorylation sites but lost all the sequences to the C terminus, including a part of the End3p binding domain and the recently identified Arp2/3 complex binding domain (Duncan *et al.*, 2001) (our unpublished results). This explains why elimination of the inhibitory phosphorylation by Prk1p improves the activity of the mutant Pan1p protein. By the same token, the *end3*Δ mutant can be suppressed by *prk1* probably because loss of End3p surrenders Pan1p to the inhibitory phosphorylation on LR2. That the *sla1*Δ mutation cannot be suppressed by *prk1*Δ suggests that protecting the LR1 region of Pan1p from the Prk1p phosphorylation is not Sla1p's main function in vivo. In agreement with this, deletion of the C-terminal repeats from Sla1p was not sufficient to generate a temperature sensitivity, whereas deleting a region near N terminus comprising the third SH3 domain was (Ayscough *et al.*, 1999). Therefore, the essential function of Sla1p is independent of its ability to interact with Pan1p.

In addition to interacting with Pan1p and End3p, Sla1p has been shown to interact with the yeast homolog of the human Wiskott-Aldrich Syndrome protein Las17p (Bee1p) (Li, 1997). The functional basis for this interaction is still unclear, because the localization of Las17p appeared to be normal in the *sla1*Δ cells (Ayscough *et al.*, 1999). On the other hand, two cortical patch-localized proteins, Sla2p and Rho1p, do require Sla1p for proper localization (Ayscough *et al.*, 1999). Furthermore, Sla1p has also been shown to interact with the translational release factor Sup35p through the C-terminal region, and may play a role in prion formation and propagation (Bailleul *et al.*, 1999). Whether these functions of Sla1p involve Pan1p is not clear at present.

Regulation by Prk1p beyond Pan1p/Sla1p/End3p Complex

Although Pan1p and Sla1p are the only two yeast proteins that contain multiple copies of the LxxQxTG motif, the ones that contain one or two copies of this motif are numerous. Interestingly, several such proteins have been shown to interact either physically or genetically with Pan1p. For example, Yap1802p, the yeast homolog of the mammalian clathrin assembly protein AP180 known to be able to interact with the EH domain of Pan1p in a two-hybrid assay (Wendland and Emr, 1998), contains one LxxQxTG motif and one QxTG motif in its Pan1p binding region. Similarly, Ent1p and Ent2p, a pair of yeast homologs of mammalian protein epsin found to be able to interact with the EH domain of Pan1p (Wendland *et al.*, 1999), both contain one LxxQxTG motif and one QxTG motif in the EH domain-binding region. Furthermore, the Sla1p interacting protein Las17p also contains one LxxQxTG motif and one QxTG motif. It will be of a great interest to see whether these proteins are also under the regulation of Prk1p.

An intricate network of protein interactions is involved in the regulation of actin cytoskeleton dynamics in yeast. Previous and present studies have provided some insights into the mechanism of how the actin dynamics is regulated. Prk1p phosphorylation on the actin patch regulatory proteins Pan1p and Sla1p to inhibit the Pan1p/Sla1p/End3p complex is likely one of the important schemes to maintain the normal function and organization of the actin cytoskeleton. There is no doubt that identification of additional upstream and downstream factors in this pathway will greatly advance our understanding of this complex cellular system.

ACKNOWLEDGMENTS

We are grateful to Hsin-yao Tang for providing numerous plasmids such as pGEX-SH3 and pPAN1c-HA, and to Alan Munn for providing the plasmid pYep352-FUR4 and the assistance with the uracil permease assay. We thank Heinrich Horstmann and Chee Peng Ng for their help with electron microscopy and Jun Wang for general technical assistance. This work was supported by the Singapore National Science and Technology Board.

REFERENCES

Adams, A.E.M., and Pringle, J.R. (1984). Relationship of actin and tubulin distribution to bud growth in wild-type and morphogenetic mutant *Saccharomyces cerevisiae*. J. Cell Biol. *98*, 934–945.

Ayscough, K.R., Eby, J.J., Lila, T., Dewar, H., Kozminski, K.G., and Drubin, D.G. (1999). Sla1p is a functionally modular component of the yeast cortical actin cytoskeleton required for correct localization of both Rho1p-GTPase and Sla2p, a protein with talin homology. Mol. Biol. Cell *10*, 1061–1075.

Ayscough, K.R., Stryker, J., Pokala, N., Sanders, M., Crews, P., and Drubin, D.G. (1997). High rates of actin filament turnover in budding yeast and roles for actin in establishment and maintenance of cell polarity revealed using the actin inhibitor Latrunculin-A. J. Cell Biol. *137*, 399–416.

Bailleul, P.A., Newnam, G.P., Teenbergen, J.N., and Chernoff, Y.O. (1999). Genetic study of interactions between the cytoskeletal assembly protein Sla1 and prion-forming domain of the release factor Sup35 (eRF3) in *Saccharomyces cerevisiae*. Genetics *153*, 81–94.

Bénédetti, H., Raths, S., Crausaz, F., and Riezman, H. (1994). The *END3* gene encodes a protein that is required for the internalization step of endocytosis and for actin cytoskeleton organization in yeast. Mol. Biol. Cell *5*, 1023–1037.

Burgess, R.R. (1991). Use of polyethyleneimine in purification of DNA-binding proteins. Methods Enzymol. *208*, 3–10.

Carlier, M.F., and Pantaloni, D. (1997). Control of actin dynamics in cell motility. J. Mol. Biol. *269*, 459–467.

Cooper, J.A., and Schafer, D.A. (2000). Control of actin assembly and disassembly at filament ends. Curr. Opin. Cell Biol. *12*, 97–103.

Cope, M.J.T.V., Yang, S., Shangand, C., and Drubin, D.G. (1999). Novel protein kinases Ark1p and Prk1p associate with and regulate the cortical actin cytoskeleton in budding yeast. J. Cell Biol. *144*, 1203–1218.

Corbalan-Garcia, S., Yang, S.S., Degenhardt, K.R., and Bar-Sagi, D. (1996). Identification of the mitogen-activated protein kinase phosphorylation sites on human Sos1 that regulate the interaction with Grb2. Mol. Cell. Biol. *16*, 5674–5682.

Dulic, V., Egerton, M., Elguindi, L., Raths, S., Singer, B., and Riezman, H. (1991). Yeast endocytosis assays. Methods Enzymol. *194*, 697–710.

Duncan, M.C., Cope, M.J., Goode, B.L., Wendland, B., and Drubin, D.G. (2001). Yeast Eps15-like endocytic protein, Pan1p, activates the Arp2/3 complex. Nat. Cell Biol. *3*, 687–690.

Dunn, B., and Wobbe, C.R. (1993). Preparation of protein extracts from yeast, p.13.13.1-13.13.9. In: Current Protocols in Molecular Biology, vol. 2, ed. F.M. Ausubel, R. Brent, R.E. Kingston, D.D. Moore, J.G. Seidman, J.A. Smith, and K. Struhl, New York: John Wiley & Sons.

Govindan, B., Bowser, R., and Novick, P. (1995). The role of Myo2, a yeast class V myosin, in vesicular transport. J. Cell Biol. *128*, 1055–1068.

Han, j., Jing, Y., Li, Z., Kravchenko, V.V., and Ulevitch, R.J. (1997). Activation of the transcription factor MEF2C by the MAP kinase p38 in inflammation. Nature *386*, 296–299.

Holtzman, D.A., Yang, S., and Drubin, D.G. (1993). Synthetic-lethal interactions identify two novel genes, *SLA1* and *SLA2*, that control membrane cytoskeleton assembly in *Saccharomyces cerevisiae*. J. Cell Biol. *122*, 635–644.

Huxley, C., Green, E.D., and Dunham, I. (1990). Rapid assessment of *S. cerevisiae* mating type by PCR. Trends Genet. *6*, 236.

Karpova, T.S., Reck-Peterson, S.L., Elkind, N.B., Mooseker, M.S., Novick, P.J., and Cooper, J.A. (2000). Role of actin and myo2p in polarized secretion and growth of *Saccharomyces cerevisiae*. Mol. Biol. Cell *11*, 1727–1737.

Kilmartin, J.V., and Adams, A.E.M. (1984). Structural rearrangements of tubulin and actin during the cell cycle of the yeast *Saccharomyces*. J. Cell Biol. *98*, 922–933.

Lew, D.J., and Reed, S.I. (1993). Morphogenesis in the yeast cell cycle: regulation by Cdc28 and cyclins. J. Cell Biol. *120*, 1305–1320.

Li, R. (1997). Bee1, a yeast protein with homology to Wiscott-Aldrich syndrome protein, is critical for the assembly of cortical actin cytoskeleton. J. Cell Biol. *136*, 649–658.

Mermall, V., Post, P.L., and Mooseker, M.S. (1998). Unconventional myosins in cell movement, membrane traffic, and signal transduction. Science *279*, 527–533.

Novick, P., and Botstein, D. (1985). Phenotypic analysis of temperature-sensitive yeast actin mutants. Cell *40*, 405–416.

Pruyne, D.W., and Bretscher, A. (2000). Polarization of cell growth in yeast. II. The role of the cortical actin cytoskeleton. J. Cell Sci. *113*, 571–585.

Pruyne, D.W., Schott, D.H., and Bretscher, A. (1998). Tropomyosin-containing actin cables direct the Myo2p-dependent polarized delivery of secretory vesicles in budding yeast. J. Cell Biol. *143*, 1931–1945.

Rose, M.D., Winston, F., and Hieter, P. (1990). Methods in Yeast Genetics: A Laboratory Course Manual, Cold Spring Harbor, NY: Cold Spring Harbor Laboratory Press.

Sachs, A.B., and Deardorff, J.A. (1992). Translation initiation requires the PAB-dependent poly(A) ribonuclease in yeast. Cell. *70*, 961–973.

Sambrook, J., Fritsch, E.F., and Maniatis, T. (1989). Molecular Cloning: A Laboratory Manual, 2nd ed., Cold Spring Harbor, NY: Cold Spring Harbor Laboratory Press.

Tang, H.Y., and Cai, M. (1996). The EH-domain-containing protein Pan1 is required for normal organization of the actin cytoskeleton in *Saccharomyces cerevisiae*. Mol. Cell. Biol. *16*, 4897–914.

Tang, H.Y., Munn, A., and Cai, M. (1997). EH domain proteins Pan1p and End3p are components of a complex that plays a dual role in organization of the cortical actin cytoskeleton and endocytosis in *Saccharomyces cerevisiae*. Mol. Cell. Biol. *17*, 4294–4304.

Tang, H.Y., Xu, J., and Cai, M. (2000). Pan1p, End3p, and Sla1p, three yeast proteins required for normal cortical actin cytoskeleton organization, associate with each other and play essential roles in cell wall morphogenesis. Mol. Cell. Biol. *20*, 12–25.

Volland, C., Urban-Grimal, D., Geraud G., and Haguenauer-Tsapis, R. (1994). Endocytosis and degradation of the yeast uracil permease under adverse conditions. J. Biol. Chem. *269*, 9833–9841.

Wendland, B., and Emr, S.D. (1998). Pan1p, yeast eps15, functions as a multivalent adaptor that coordinates protein-protein interactions essential for endocytosis. J. Cell Biol. *141*, 71–84.

Wendland, B., Steece, K.E., and Emr, S.D. (1999). Yeast epsins contain an essential N-terminal ENTH domain, bind clathrin and are required for endocytosis. EMBO J. *18*, 4383–4393.

Zeng, G., and Cai, M. (1999). Regulation of the actin cytoskeleton organization in yeast by a novel serine/threonine kinase Prk1p. J. Cell Biol. *144*, 71–82.

Zhao, Z.S., Manser, E., and Lim, L. (2000). Interaction between PAK and Nck: a template for Nck targets and role of PAK autophosphorylation. Mol. Cell. Biol. *20*, 3906–3917.